Nanoscale

Cite this: *Nanoscale*, 2011, **3**, 3627

www.rsc.org/nanoscale

COMMUNICATION

Highly effective SERS substrates based on an atomic-layer-deposition-tailored nanorod array scaffold†

Monan Liu, Li Sun, Chuanwei Cheng, Hailong Hu, Zexiang Shen and Hong Jin Fan*

Received 10th June 2011, Accepted 20th July 2011
DOI: 10.1039/c1nr10595g

When two metallic surfaces supporting plasmonic excitation are brought into close proximity of each other, a nanogap (of width on the subwavelength scale) will form, which boosts greatly the local optical field. Based on this idea, we fabricated two types of three-dimensional plasmonic substrates with such nanogaps, taking advantage of both atomic layer deposition (ALD) and the capillary effect. Owing to the counteraction of the gap-reducing and capillary, nanogaps with different widths and profiles have been formed on the scaffold of aligned ZnO nanorods and shown to induce large field enhancement with enhancement factor up to 2.64 × 10^6 for surface-enhanced Raman scattering (SERS).

I. Introduction

Plasmonic functionalization based on metallic modification *via* various methods has proved to be universally effective for optical field enhancement,[1–3] irrespective of the chosen metal species or the resulting surface morphologies. The enhanced optical field can be a key motivation for a variety of advanced applications and devices, such as near-field scanning optical microscopy,[4,5] photodetectors,[6,7] nanolasers,[8] photovoltaics[9,10] and catalysis.[11] Distinguished by their frequency dependence, metal structures for plasmonic-light concentration can be either resonant or non-resonant. Resonant structures, such as single subwavelength particles or their fractal aggregates, have been shown to enhance the local field by at least one order of magnitude.[12] Non-resonant effects, such as "feed-gaps"[13] and "lightning rods",[14] are often considered for more delicate concentrators to achieve a broadband field enhancement[15], both taking advantage of dielectric contrast-based enhancement. In particular, a feed-gap is known as a thin gap inserted into metallic structures, which enables strongly-localized plasmonic field distribution within the gap.[16] Very recently, this feed-gap effect has been brought forward to the forefront of plasmonic structure design again, as highlighted by the deep-subwavelength-scale plasmon photonic devices.[8,17–21]

To fine tune the gap between tiny metal particles, one possible way is having them well-distributed on two "fingers" first, which are then brought closer and closer until the separation distance down to the deep-subwavelength scale so as to form a real "nano-gap".[22,23] Actually, a similar process occurs inherently due to the capillary effect for aligned nanostructures with metal capping.[22–25] In the presence of an enhanced optical field within the nanogaps, these structures have shown great potential as 3-D SERS substrates.[22–24] Among all such structures, vertically aligned ZnO nanorods (NRs) grown on sapphire substrate are especially ideal for developing advanced surface-enhanced Raman scattering (SERS) substrates due to their good flexibility and easily-tuned array density (free of additional lithography step).

In this Communication, we succeeded in fine tuning the gap distance between vertically aligned ZnO nanorods and realize plasmonic nanogaps packed with 3-D SERS substrates on whole-template-scale with good control in both the nanostructure and enhancement strategy. Atomic layer deposition (ALD) was employed to narrow precisely the gap between adjacent NRs (*i.e.* the gap between proximate Ag particles from two NRs). In particular, two types of gap profiles are realized intentionally by balancing two competing synthetic factors: ALD thickening and the capillary effect. Subsequently, this simple method allows the formation of two types of substrate structures, both exhibiting strong field concentrations.

II. Experimental

Sample preparation

Well-aligned ZnO NR arrays were grown on *a*-plane sapphire substrates *via* chemical vapor deposition with thoroughly mixed ZnO and graphite powders as source material. The growth details can be found in a previous publication.[26] The as-grown samples were cut into small pieces for the subsequent depositions of ALD coating and Ag sputtering. The gap-tuning layers of amorphous ZnO were coated by ALD, in which various ALD cycles were chosen for the thickness of 10, 20, 40, 50 and 60 nm, respectively. The thickness control was based on a pre-calibration curve which shows the standard linear dependence of thickness on cycle number. The outer layers of Ag were coated *via* DC sputtering (JFC-1600, JEOL). The sputtering was performed under a fixed current control of 10 mA for 40 s. Some samples were directly sputtered with Ag without the middle ZnO gap-tuning layer as a control experiment. The morphology of the NRs was observed using both the scanning electron microscope (SEM) and transmission electron microscope (TEM). For molecule

Division of Physics and Applied Physics, School of Physical and Mathematical Sciences, Nanyang Technological University, 21 Nanyang Link, 637371, Singapore. E-mail: fanhj@ntu.edu.sg

† Electronic supplementary information (ESI) available. See DOI: 10.1039/c1nr10595g

loading, all the prepared samples were dipped in an aqueous solution of R6G molecules with a concentration of 5×10^{-5} M for 20 min. They were then washed three times with deionized water and left in a dark room until dried naturally in air. The loading process was performed immediately before optical characterization.

Optical characterizations

The reflectance spectra were measured on a Zolix Solar Cell Scan100 IPCE measurement system, equipped with a 150 W Xeon lamp as the light source. The SERS measurements were carried out on a WITEC CRM200 Raman system with a 532 nm line laser as excitation. The beam size of the laser is about 1 μm in diameter and the incident power was set to be 20 μW. At least three measurements were taken by selecting different detecting spots on each sample to ensure the reproducibility. All the Raman spectra were obtained at room temperature with the same accumulation time and incident power.

III. Results and discussions

Fig. 1 shows SEM images of both as-grown ZnO NRs and plasmonic SERS substrates undergoing 20 min dipping in an aqueous solution of R6G molecules (molar concentration 5×10^{-5} M). Fig. 1(a) confirms the good alignment of as-grown ZnO NRs, which ensures both subsequent the gap-tuning and conformal metal-deposition (with Fig. 1(b) showing the capillary effect of these scaffold NRs). Fig. 1(c) to (h) sum up the overall scaffold morphology of the plasmonic 3-D substrates with increasing ALD layer thickness (0, 10, 20, 40, 50, 60 nm), for which the capped Ag nanoparticles were deposited under the very same sputtering conditions. Here ZnO NRs directly capped with Ag were chosen as a reference to show how they perform as a SERS substrate with the original scaffold morphology before gap-tuning. The ZnO layer as-deposited by ALD is multicrystalline and works as a dielectric environment for the nanogap between adjacent NRs while tuning its width. The resulting plasmonic coating of Ag can be identified as a layer of percolated nanoparticles by zoomed-in images (c) to (h). Optical absorption measurement did not show an evident plasmonic peak of Ag, probably due to their small sizes (see ESI†).

To learn the substrate structure, first, it can be observed that the scaffold morphologies of sample (b) to (e) are all "bundled" NRs induced by the capillary effect while dipped into an aqueous solution of R6G (*i.e.*, proximate NR tips attracted to each other by capillary force). This is a common phenomenon for 3-D SERS substrates, such as nanowires,[24] nanotubes[23] and nanofingers.[22] However, with the further thickening of the NRs (thicker ALD layer), this capillarity-induced bundling in turn is found to be suppressed. The suppression is represented by a "looser bundling" between proximate NRs [image (e)], as a result of poor flexibility of the NR body due to thicker ALD coating. Owing to counteractive gap-tuning ALD coating and the capillary effect, SERS substrates of densely-bundled NRs can be acquired with extremely thin gaps of wedge-like profile. In this strategy, it is known that optical field can be focused into the nanogaps between tapped NR tips.[22,23] We noted that the substrate with 10 nm ALD layer possesses the thinnest nanogap (average width below 10 nm) and hence has the greatest expectation for plasmonic concentration.[23] Then, when the coating thickness is increased up to 40 nm and above (images (f) to (h)), the bundles almost disassemble and the NRs return to a quasi-aligned structure. In this case, uniform nanogaps instead of wedge-like ones are formed and hence will support field enhancement over large area along the thin long gap profile, as simulated in previous publications.[23,27]

As a summary on the substrate structure evolution, by introducing an ALD layer to further reduce the gap width between proximate NRs, two kinds of SERS substrate structure have been obtained, *viz.*, bundled and quasi-aligned (as shown in the schematic in Fig. 2), both with nanogaps down to 10 nm and below. Furthermore, the metal–nanogap–metal structure formed in this way is well-surrounded by a dielectric environment (multicrystalline ALD ZnO layer, dielectric constant ~6.0 [ref. 28]; other alternative ALD dielectric layers such as alumina can also be used here). This is the key feature distinguishing our SERS substrates from most reported ones, as the ALD dielectric layer contributes to preventing the excited SPs' loss into the direct-band semiconductor scaffold.

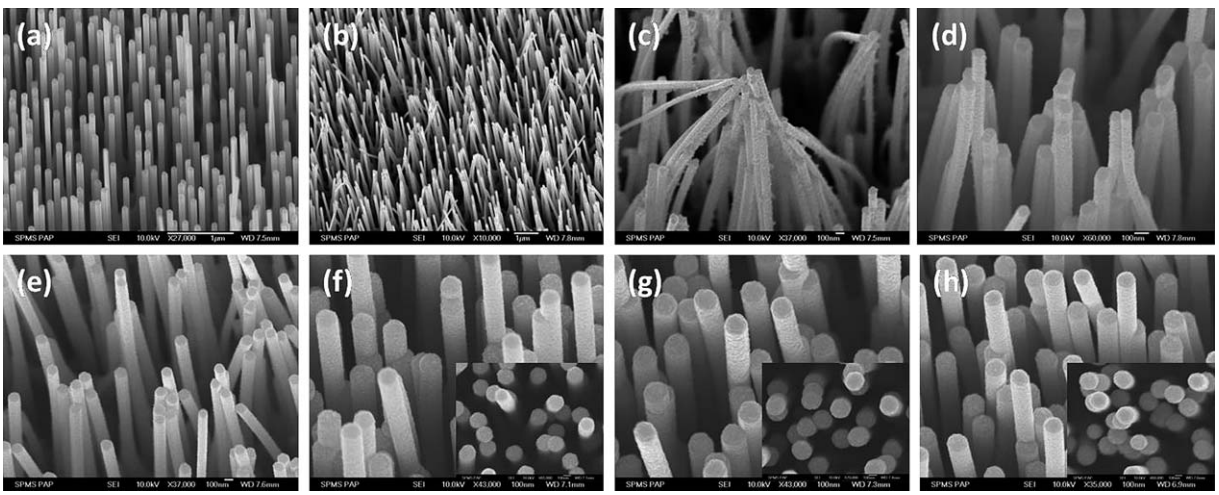

Fig. 1 SEM images of the nanorod scaffold plasmonic SERS substrates: (a) as-grown vertically aligned ZnO NRs as the starting scaffold; (b) capillary scaffold of these pristine ZnO NRs; and (c) ZnO-Ag; (d) ZnO(+10)-Ag; (e) ZnO(+20)-Ag; (f) ZnO(+40)-Ag; (g) ZnO(+50)-Ag; (h) ZnO(+60)-Ag as plasmonic SERS substrates. Numbers in the parentheses denote the ALD coating thickness. Insets in images (f–h) show the top view of the quasi-aligned structure. The definition for the quasi-aligned and bundle structure can be found in the text.

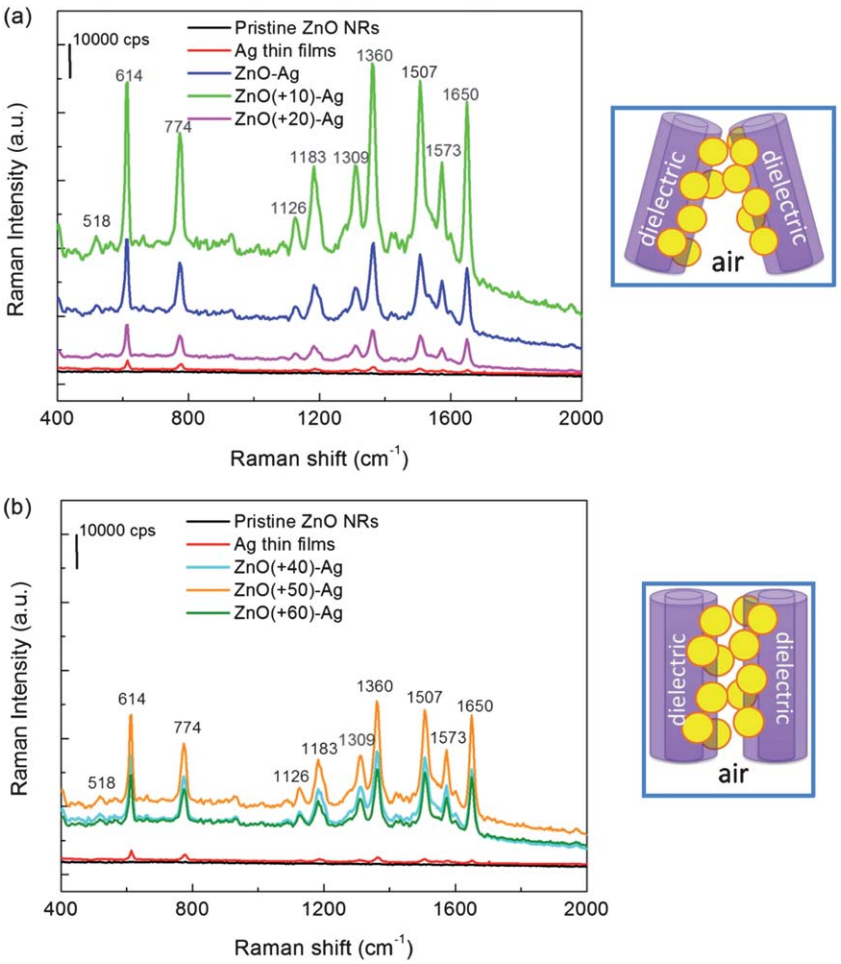

Fig. 2 SERS spectra of R6G molecules with a concentration 5×10^{-5} M, collected from (a) bundled structure and (b) quasi-aligned structure, respectively. Both spectra include the results from two reference samples: pristine ZnO NRs and Ag thin films.

Fig. 2 shows the SERS results of R6G molecules (molar concentration 5×10^{-5} M) dispersed on all the modified substrates, with that on pristine ZnO NRs and Ag thin films as references (no R6G related Raman signal can be observed on the pristine NR scaffold). All the Raman bands match well with those of the characteristic spectrum of R6G as follows.[29] The bands at 1360, 1507, 1573 and 1650 cm^{-1} are assigned to C–C stretching modes and those at 1126 and 1183 cm^{-1} are assigned to C–H in-plane bending modes. Furthermore, the bands at 518, 614, 774 and 1309 cm^{-1} are assigned to the torsional and/or bending, C–C–C in-plane bending, C–H out-of-plane bending and C–O–C stretching modes, respectively. By comparing the peak intensities between different substrates, it can be found that both substrate structures (bundled and quasi-aligned) have intensively enhanced the Raman signal, indicating that the narrowed gap is highly effective for plasmonic concentration, and hence optical field enhancement. For evaluating the nanogap effect, these field enhancement results should be compared based on their own gap profile. For bundled structure [Fig. 2(a)], the narrowed nanogaps all have wedge-like-profiles but with different wedge angles and gap widths. By comparing images (c), (d) and (e) in Fig. 1, it's evident that the substrate ZnO(+10)-Ag (ZnO NRs with 10 nm coating) possesses a much tighter bundling than ZnO-Ag and ZnO(+20)-Ag substrates, *i.e.* the smallest wedge angle and gap width (estimated to be 5° and 5 nm on average). As shown by Dawson *et al.* previously,[23] for such wedge-like-profiled nanogaps between plasmonic layers, a reduced gap width can greatly boost the local field intensity, with an enhancement ratio up to 180 and above within a single gap. Therefore, in this concentration strategy, the enhanced Raman signal can be well ascribed to the notable gap width difference between the three modified substrates, whose intensities follow the gap-width relationship inversely: ZnO(+10)-Ag > ZnO-Ag > ZnO(+20)-Ag. For quasi-aligned structure (Fig. 2(b)), all the three substrates also give strong enhancement to the Raman signal, with the relationship ZnO(+50)-Ag > ZnO-Ag(+40) > ZnO(+60)-Ag. The basic trend here is still that the signal enhancement follows gap width inversely, and hence proves that the nanogap effect for plasmonic field concentration works for both gap profiles. Note that the thickest ALD coating of 60 nm fails to bring the strongest enhancement in this strategy. This is most likely because when the NRs become too densely packed, the gaps between them can be too small for loading Ag nanoparticles during the sputtering process and hence reduce the total signal intensity.

To further show the nanogap effect on plasmonic concentration, the enhancement factors (EFs) of the SERS results have been estimated based on the following formula,[30]

$$EF = (I_{SERS}/I_{bulk})/(C_{SERS}/C_{bulk})$$

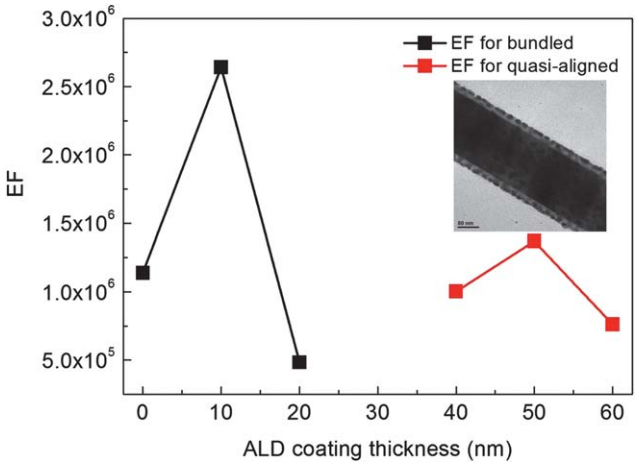

Fig. 3 Ehancement factor (EF) due to narrowed nanogap plotted *vs.* ALD layer thickness. Inset shows a TEM image of a single ALD thickened NR with Ag nanoparticle capping.

where I_{SERS} and I_{bulk} stand for the SERS and bulk Raman peak intensities while C_{SERS} and C_{bulk} for the molar concentration of R6G molecules in the aqueous solution used in the dipping step and that of R6G bulk sample, respectively. The characteristic band at 1507 cm^{-1} was chosen for the EF estimation. In this way, the EFs have been calculated and plotted *versus* ALD coating thickness, as shown in Fig. 3. From the plot, it can be seen that both kinds of SERS substrates can offer large field enhancement to the Raman signal, with overall EF above 5×10^5 and up to 2.64×10^6. This means the proposed method for obtaining deeply-reduced nanogaps with dielectric environment is very effective for plasmonic field concentration. Such nanogaps benefit not only from the further compressed width but also from the dielectric contrast at the metal-to-air interface, as required by the boundary conditions.[16] Moreover, the surrounding dielectric environment also serves as a shelter that reduces the scattering of the incident light to the scaffold.[31] This ensures the enhanced optical field can effectively contribute to the Raman signal. All these factors make the dielectric-surrounded nanogap a distinctive plasmonic concentration structure. Meanwhile, while quasi-aligned structures so far do not give an EF larger than bundled ones; it should be noted that the former can actually induce a medium field enhancement along the gap profile rather than focus the field to the "wedge tip" (which is the case for bundled structures). This means that such global field enhancement within the 3-D substrates may show great potential in other plasmonic devices or applications, taking advantage of both the large surface area and the enhanced local field.

Conclusion

A very simple method based on ZnO nanorod arrays as the template was applied to fabricate plasmonic nanogap substrates, which prove to be highly efficient SERS substrates with an estimated enhancement factor up to 2.64×10^6. The key point of this work is that the nanogaps are realized based on fine thickness tuning *via* atomic layer deposition (ALD) and the nanorod capillary effect, resulting in either bundled or quasi-aligned column structures. As a consquence of the nanogap size effect, the field enhancement depends critically on the ALD thickness and the structure profile. Our future work includes using a well-ordered nanorod scaffold for more accurate estimation of the molecules' concentration, and extending the ALD ZnO dielectric layer to other higher-k materials such as Al_2O_3 and ZrO_2.

References and notes

1 S. A. Maier and H. A. Atwater, *J. Appl. Phys.*, 2005, **981**; S. A. Maier and H. A. Atwater, *J. Appl. Phys.*, 2005, **98**, 011101.
2 Y. N. Xia and N. J. Halas, *MRS Bull.*, 2005, **30**, 338–344.
3 J. Aizpurua, G. W. Bryant, L. J. Richter, F. J. G. de Abajo, B. K. Kelley and T. Mallouk, *Phys. Rev. B: Condens. Matter Mater. Phys.*, 2005, **71**.
4 W. Srituravanich, L. Pan, Y. Wang, C. Sun, D. B. Bogy and X. Zhang, *Nat. Nanotechnol.*, 2008, **3**, 733–737.
5 T. H. Taminiau, R. J. Moerland, F. B. Segerink, L. Kuipers and N. F. van Hulst, *Nano Lett.*, 2007, **7**, 28–33.
6 T. Ishi, J. Fujikata, K. Makita, T. Baba and K. Ohashi, *Jpn. J. Appl. Phys.*, 2005, **44**, L364–L366.
7 L. Tang, S. E. Kocabas, S. Latif, A. K. Okyay, D. S. Ly-Gagnon, K. C. Saraswat and D. A. B. Miller, *Nat. Photonics*, 2008, **2**, 226–229.
8 R. F. Oulton, V. J. Sorger, T. Zentgraf, R. M. Ma, C. Gladden, L. Dai, G. Bartal and X. Zhang, *Nature*, 2009, **461**, 629–632.
9 T. Kume, S. Hayashi, H. Ohkuma and K. Yamamoto, *Jpn. J. Appl. Phys.*, 1995, **34**(Part 1, No. 12A), 6448–6451.
10 O. Stenzel, A. Stendal, K. Voigtsberger and C. Vonborczyskowski, *Sol. Energy Mater. Sol. Cells*, 1995, **37**, 337–348.
11 W. H. Hung, M. Aykol, D. Valley, W. B. Hou and S. B. Cronin, *Nano Lett.*, 2010, **10**, 1314–1318.
12 M. I. Stockman, V. M. Shalaev, M. Moskovits, R. Botet and T. F. George, *Phys. Rev. B: Condens. Matter*, 1992, **46**, 2821–2830.
13 P. J. Schuck, D. P. Fromm, A. Sundaramurthy, G. S. Kino and W. E. Moerner, *Phys. Rev. Lett.*, 2005, **94**.
14 E. Verhagen, M. Spasenovic, A. Polman and L. Kuipers, *Phys. Rev. Lett.*, 2009, **102**.
15 M. I. Stockman, *Phys. Rev. Lett.*, 2004, **93**.
16 T. Sondergaard and S. I. Bozhevolnyi, *Opt. Express*, 2007, **15**, 4198–4204.
17 D. R. Ward, F. Huser, F. Pauly, J. C. Cuevas and D. Natelson, *Nat. Nanotechnol.*, 2010, **5**, 732–736.
18 P. Spinelli, M. Hebbink, R. de Waele, L. Black, F. Lenzmann and A. Polman, *Nano Lett.*, 2011, **11**, 1760–1765.
19 O. L. Muskens, V. Giannini, J. A. Sanchez-Gil and J. G. Rivas, *Nano Lett.*, 2007, **7**, 2871–2875.
20 M. Schnell, A. Garcia-Etxarri, A. J. Huber, K. Crozier, J. Aizpurua and R. Hillenbrand, *Nat. Photonics*, 2009, **3**, 287–291.
21 D. K. Lim, K. S. Jeon, H. M. Kim, J. M. Nam and Y. D. Suh, *Nat. Mater.*, 2009, **9**, 60–67.
22 M. Hu, F. S. Ou, W. Wu, I. Naumov, X. M. Li, A. M. Bratkovsky, R. S. Williams and Z. Y. Li, *J. Am. Chem. Soc.*, 2010, **132**, 12820–12822.
23 P. Dawson, J. A. Duenas, M. G. Boyle, M. D. Doherty, S. E. J. Bell, A. M. Kern, O. J. F. Martin, A. S. Teh, K. B. K. Teo and W. I. Milne, *Nano Lett.*, 2011, **11**, 365–371.
24 L. M. Chen, L. B. Luo, Z. H. Chen, M. L. Zhang, J. A. Zapien, C. S. Lee and S. T. Lee, *J. Phys. Chem. C*, 2010, **114**, 93–100.
25 C. W. Cheng, B. Yan, S. M. Wong, X. L. Li, W. W. Zhou, T. Yu, Z. X. Shen, H. Y. Yu and H. J. Fan, *ACS Appl. Mater. Interfaces*, 2010, **2**, 1824–1828.
26 C. W. Cheng, B. Liu, E. J. Sie, W. W. Zhou, J. X. Zhang, H. Gong, C. H. A. Huan, T. C. Sum, H. D. Sun and H. J. Fan, *J. Phys. Chem. C*, 2010, **114**, 3863–3868.
27 X. Wen, *et al.*, *Nanotechnology*, 2011, **22**, 085203.
28 C. F. Herrmann, F. W. DelRio, D. C. Miller, S. M. George, V. M. Bright, J. L. Ebel, R. E. Strawser, R. Cortez and K. D. Leedy, *Sens. Actuators, A*, 2007, **135**, 262–272.
29 P. Hildebrandt and M. Stockburger, *J. Phys. Chem.*, 1984, **88**, 5935–5944.
30 S. L. Smitha, K. G. Gopchandran, T. R. Ravindran and V. S. Prasad, *Nanotechnology*, 2011, **22**, 265705.
31 J. Mertz, *J. Opt. Soc. Am. B*, 2000, **17**, 1906–1913.

